ORIGINAL ARTICLE

Correlation Between Wall Shear Stress and Acute Degradation of the Endothelial Glycocalyx During Cardiopulmonary Bypass

Guoliang He[1] · **Yuan Gao**[1] · **Linya Feng**[1] · **Guodong He**[1] · **Qiaolin Wu**[1] · **Wei Gao**[1] · **Lina Lin**[1] · **Weijian Wang**[1]

Abstract

Wall shear stress (WSS) plays a key role in maintaining glycocalyx function, gene expression, and structure. Experimental studies have discussed the relationship between the shedding of the endothelial glycocalyx (EG) and WSS. However, rare literature about how WSS affects the EG during cardiopulmonary bypass (CPB) was mentioned. This study aimed to investigate the correlation between the WSS of carotid arteries and shedding of the EG during CPB in humans. The WSS level was calculated in accordance with an equation. The plasma concentrations of heparan sulfate, syndecan-1, and nitric oxide were measured to reflect shedding of the EG at six time points. A negative correlation was observed between the peak wall shear stress (PWSS) and syndecan-1 ($R = -0.5$, $p < 0.01$) and heparan sulfate ($R = -0.461$, $p < 0.01$) during CPB. The WSS is closely associated with the components of glycocalyx shedding during CPB. The WSS produced by non-pulsatile flow during CPB may contribute to the degradation of EG.

Abbreviations

WSS	Wall shear stress
PWSS	Peak wall shear stress
MWSS	Mean wall shear stress
EG	Endothelial glycocalyx
CPB	Cardiopulmonary bypass
HS	Heparan sulfate
NO	Nitric oxide
ECG	Electrocardiogram
ICU	Intensive care unit
SIRS	Systemic inflammatory reaction syndrome

Associate Editor Junjie Xiao oversaw the review of this article

Electronic supplementary material The online version of this article (https://doi.org/10.1007/s12265-020-10027-2) contains supplementary material, which is available to authorized users.

✉ Weijian Wang
  wangwj2002@hotmail.com

✉ Lina Lin
  wzlinlina@163.com

1 Department of Anesthesiology, The First Affiliated Hospital of Wenzhou Medical University, Wenzhou 325000, Zhejiang, China

Introduction

EG is a polysaccharide-rich, villous cell structure that covers the luminal side of vascular endothelial cells. Its main components include glycosaminoglycan chains (chondroitin sulfate, heparin sulfate, and hyaluronic acid), proteoglycans (syndecan and glypican families), membrane glycoproteins, and related plasma proteins [1]. Studies on intact EG have revealed several critical functions that maintain vascular permeability [2] and the regulation of anti-inflammatory responses [3], reduction of platelet count, and leukocyte adhesion [4]. Moreover, the glycocalyx, as a mechanosensor, is involved in mediating flow-induced shear stress and transforms into endothelial cytoskeleton [5–7].

A stable WSS can promote the synthesis of glycocalyx [8]. By contrast, a low WSS would cause degradation of the glycocalyx [9, 10]. The EG maintains balance between biosynthesis and degradation by stable WSS [11]. Most studies on the effect of flow shear stress-induced changes in glycocalyx have been carried out in vitro [12–14].

Extensive research has confirmed that glycocalyx shedding is detected during CPB. The levels of syndecan-1 and heparan sulfate significantly increase after CPB [15–17]. Furthermore,

Springer

Assmann et al. [18] reported that a non-pulsatile perfusion during CPB could result in generally decreased peak blood flow speed and reduced PWSS. However, rare clinical literatures have found to prove the relationship between glycocalyx shedding and WSS of carotid arteries during CPB.

In this study, we aimed to investigate the correlation between the WSS of the carotid arteries and degradation of glycocalyx during CPB. We used ultrasound to measure the carotid blood wall shear rate.

Materials and Methods

Study Design

The study protocol was reviewed by our institutional review board and approved as a prospective study (approval number: 2016056). Informed consent was obtained from each patient. A total of 38 patients undergoing elective cardiac surgery with extracorporeal circulation in the First Affiliated Hospital of Wenzhou Medical University from October 2016 to March 2017 were enrolled. The exclusion criteria are as follows: patients aged < 18 or > 70 years, with carotid artery stenosis > 50% or presence of plaque(s), undergoing reoperation or emergency surgery, with New York Heart Association (NYHA) Class IV cardiac function, with atrial fibrillation, and who refused to participate.

Anesthesia

General anesthesia was induced with intravenous etomidate (0.2 mg/kg), midazolam (0.4 mg/kg), sufentanil (2 μg/kg), and vecuronium (0.1 mg/kg) and maintained with sevoflurane (1.5–2.5 vol%), propofol, and vecuronium. Arterial and central venous catheters were placed after induction of anesthesia.

Surgical Procedures

After median sternotomy, all patients received systemic heparinization (400 IU/kg) before aortic artery cannulation. Next, bicaval cannulation was performed, and cardiopulmonary bypass was initiated. A cardiac index of 2.0–2.6 L/min/m^2 was maintained in all patients, and when pulsed flow was administered, a fixed rate of 80 beats/min with an augmentation of 50%, which generated a sinusoidal flow pattern, was applied throughout aortic cross-clamping.

Ultrasound Measurement of Blood Flow Velocity (V) and Diameter (D) in the Carotid Arteries

The diameters of the arterial images were obtained using an ultrasound machine (ProSound α6, ALOKA, Inc., Tokyo, Japan). The measurement site was 2 cm anterior to the left carotid sinus. A color Doppler ultrasound system and linear array high-frequency probes (frequency 5–8 MHz) were used. The measuring technician had been trained in vascular ultrasound measurements. To prevent deviations due to measurements at multiple time points, we established a self-made cervical arc on the patients' head and neck. Spectral Doppler was used for the measurement of flow velocity. The sample volume was placed in the center of the lumen. The sample volume was 2/3 of the lumen diameter. The ultrasound measurement included the angle between the sound beam and the blood flow. When the angle was less than 60°, or when the included angle line was parallel to the blood vessels, the electrocardiogram (ECG) monitor was connected. M-mode ultrasound measurement was used for measuring the diameter, and the end-diastolic inner vessel diameter at the trigger point of R-wave in the ECG was measured. The velocity of three consecutive cardiac cycles was used (Fig. 1). The velocity and diameter of the carotid arteries were measured at six time points: before surgery (T1), 10 min after the initiation of CPB (T2), at the end of CPB (T3), 15 min after unclamping the aorta (T4), 1 day after surgery (T5), and 5 days after surgery (T6).

Measurement of Whole Blood Viscosity (μ)

At each time point, 2 ml blood was drawn from the left radial artery of the patient. The measurement was completed within 30 s by using a hemorheology meter (SA-5000, Succeeder, Inc., Beijing, China).

Determination of Wall Shear Stress

The WSS was predicted by assuming the Poiseuille or Womersley flow. Pulsatile flow behavior is accurately described by the Womersley model [19]. In this study, the Poiseuille model was used to measure the mean wall shear stress (MWSS), and the Womersley model was used to measure the peak wall shear stress (PWSS). Both models were used to predict the WSS based on centerline velocity [20]. For Poiseuille flow, the predicted value can be calculated as follows:

$$MWSS = \frac{4v}{D} \cdot \mu \tag{1}$$

Womersley described the flow caused by a pulsatile pressure gradient. To calculate the Womersley flow, we decomposed the measured centerline velocity and flow rate into their Fourier components. The harmonics of heart rate (beats/min) is a dimensionless number that describes the relationship of inertial to viscous forces:
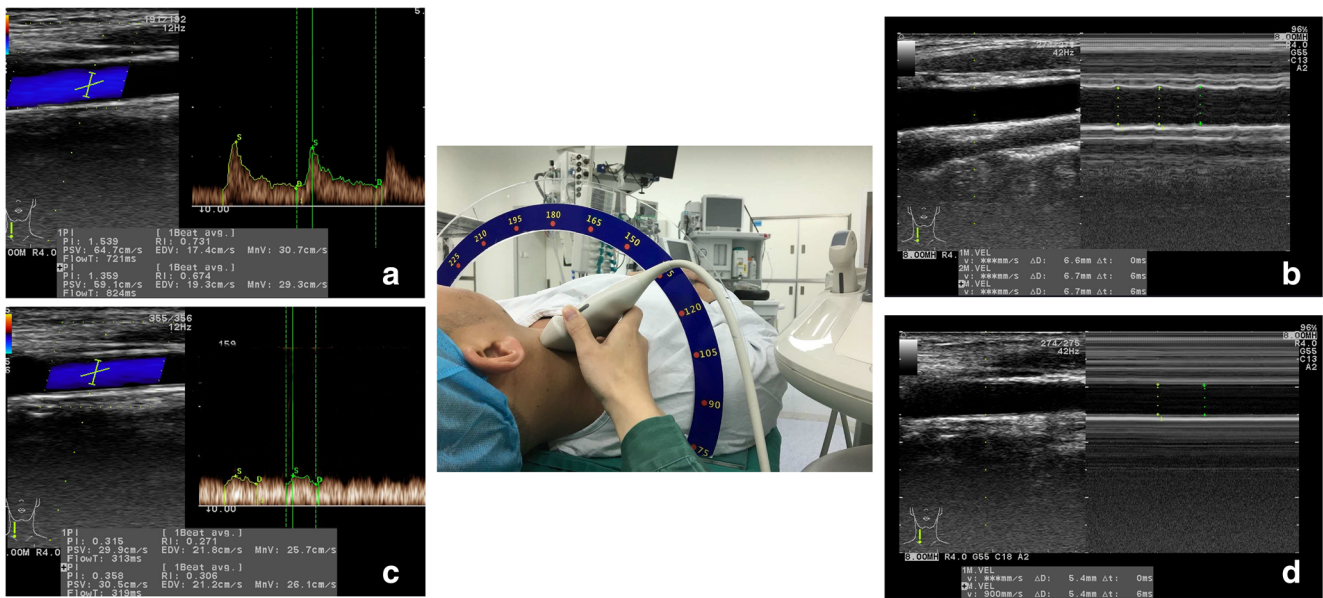
Fig. 1 Ultrasonographic measurement of blood flow velocity and vessel diameter of the carotid arteries before and after CPB (**a** and **c**, respectively). Ultrasonographic measurement of blood flow velocity and vessel diameter of the carotid arteries during CPB (**b** and **d**, respectively).

$$a = R\sqrt{\frac{\omega.\rho}{\mu}} \tag{2}$$

$$b_n = a_n i^{3/2} \tag{3}$$

$$PWSS(t) = \frac{2\mu}{R}.v_0(t) - \frac{\mu}{R}\sum_{\substack{n=30\\n\neq0}}^{30} k\left(\frac{J_1\,(b_n)}{J_0\,(b_n)-1}.v_n(t)\right) \tag{4}$$

where μ is the blood viscosity, R is the radius of the vessel, $v(0, t)$ is the centerline velocity, ρ is the fluid density, ω is the angular frequency of the driving pressure gradient, J_n is a Bessel function of order n, and k denotes that only the real part is obtained [21].

Measurement of Syndecan-1, Heparan Sulfate (HS), and Nitric Oxide (NO) Concentrations in Blood Plasma

The concentrations of syndecan-1, HS, and NO were determined directly from the plasma by using an enzyme-linked immunosorbent assay kits. The kits used horseradish peroxidase-conjugated monoclonal antibodies against human syndecan-1, HS, and NO (Shanghai Westang Co., Shanghai, China).

Statistical Analyses

Normally distributed data (evaluated by Kolmogorov–Smirnov tests) are presented as mean ± SD, and non-normally distributed data are presented in terms of the median (interquartile range). Data were analyzed for statistical difference using the Friedman repeated measures analysis of variance on ranks followed by the Wilcoxon tests as appropriate.

Changes in WSS were tested using the Wilcoxon signed rank test. Linear correlations between the plasma concentrations of glycocalyx markers and the values of WSS were calculated through the Spearman correlation test. Changes were considered statistically significant if $p < 0.05$.

Results

Clinical Characteristics

A total of 38 patients undergoing cardiac operations were enrolled in this study. Table 1 lists the data on their characteristics.

Plasma Concentrations of Syndecan-1, HS, and NO

The baseline values of syndecan-1, HS, and NO of patients in the present study achieved median values of 1.05 (0.81–1.21) and 565 (479–728) µg/dL and 67.23 (40.56–83.21) µM, respectively. The plasma syndecan-1 level of the patients increased after CPB (T2) ($p < 0.01$) and reached its peak at 15 min after unclamping the aorta (T4) ($p < 0.01$). The value obtained was equivalent to approximately 10 times the baseline level T1 ($p < 0.01$) and decreased gradually to the preoperative level after surgery. The plasma HS concentration increased at T2 ($p > 0.05$) and reached its peak at T4 ($p < 0.01$). The value was equivalent to 1.9 times of the baseline level. The plasma NO concentration decreased at T2 ($p < 0.01$) and reached its trough at T4 ($p < 0.01$). The acquired

Table 1 Characteristics and risk factors of the study patients

Characteristic	Value
Patient	
Age (years)	53 ± 11
Male (%)	65.8 (25)
Body mass index (kg/m^2)	22.7 ± 3.6
Systolic blood pressure (mmHg)	125 ± 11
Diastolic blood pressure (mmHg)	71 ± 12
Total cholesterol (mmol/L)	4.3 ± 1.2
Triglycerides (mmol/L)	1.5 ± 0.7
HDL cholesterol (mmol/L)	1.1 ± 0.4
LDL cholesterol (mmol/L)	2.8 ± 0.7
Diabetes mellitus (%)	13.2 (5)
Any history of cigarette smoking (%)	26.3 (10)
ACE inhibitor treatment (%)	21.1 (8)
Nitrate treatment (%)	42.1 (16)
Calcium blocker treatment (%)	31.5 (12)
Surgical	
CABG, % (n)	50 (19)
Valvular operation, % (n)	50 (19)
Operation time (h)	4.5 ± 1.1
Bypass time (min)	128.8 ± 41.1
Aortic clamping time (min)	90.6 ± 35.2

value was equivalent to approximately 0.5 times the baseline level and increased sharply at T5 (Fig. 2).

Calculated Peak and Mean Wall Shear Stress

Figure 3 shows the calculated PWSS and MWSS values. The baseline values of the PWSS and MWSS in the present study achieved medians of 22.94 (17.64–32.35) and 10.01 (8.43–14.21) 2dys/cm^2, respectively. The PWSS of the carotid arteries declined at T2 ($p < 0.01$) and reached its trough after starting the cardiopulmonary bypass ($p < 0.01$). After the recommencement of heartbeats, pulsatile blood flow resumed in the carotid arteries, and the PWSS gradually increased ($p < 0.01$) but did not return to the preoperative level at 5 days after surgery. The MWSS showed the same fluctuations. The MWSS in T3 significantly differed with that in T1. During the time period from the clamping to the unclamping of the aorta, the WSS was measured continuously every 15 min, in which the WSS remained stable (Fig. 3).

Correlations of the Peak and Mean Wall Shear Stress with HS, NO, and Syndecan-1 During Cardiopulmonary Bypass

The PWSS was positively correlated with NO ($R = 0.401$, $p < 0.01$) and negatively correlated with syndecan-1 ($R = -0.5$, $p < 0.01$) and HS ($R = -0.461$, $p < 0.01$).

A relatively weak correlation was observed between MWSS and serum markers. The MWSS was positively correlated with NO ($R = 0.394$, $p < 0.01$) and negatively correlated with syndecan-1 ($R = -0.427$, $p < 0.01$) and HS ($R = -0.430$ $p < 0.01$) (Fig. 4).

Correlations of Aortic Clamping Time with HS and Syndecan-1

The aortic clamping time during cardiopulmonary bypass was positively correlated with peak plasma Δsyndecan-1 (plasma levels of T4–T1 syndecan-1; $R = 0.545$, $p < 0.01$) and ΔhHS (plasma levels of T4–T1 HS; $R = 0.551$, $p < 0.01$) concentrations (Fig. 5).
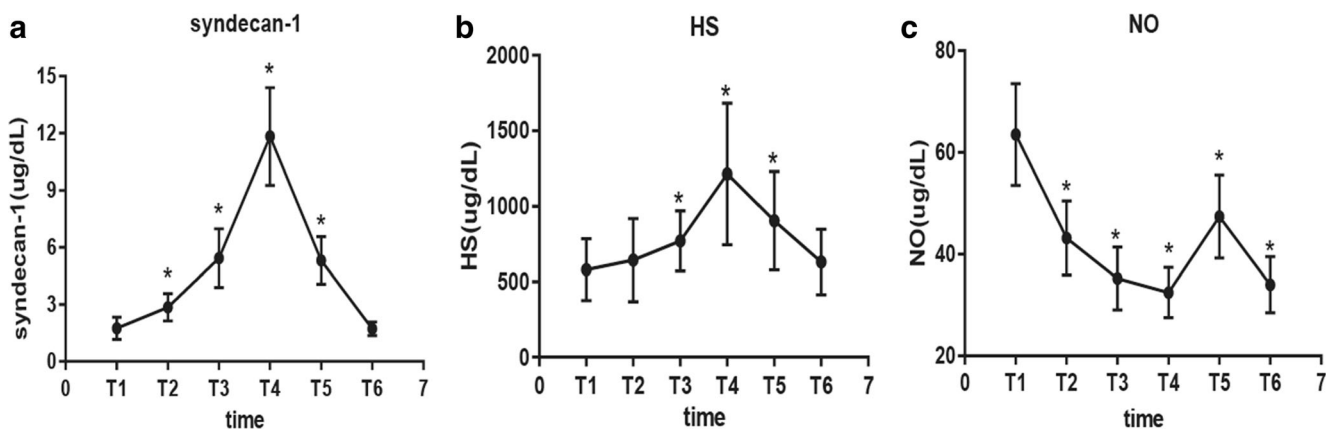
Fig. 2 Individual and median fold change of normalized syndecan-1 (CD 138), heparan sulfate (HS), and nitric oxide (NO) concentrations at different operative stages. Individual syndecan-1, heparan sulfate, and nitric oxide concentrations were determined in relation to the individual total protein concentration to account for hemodilution. **a** Syndecan-1 variation diagram. **b** Heparan sulfate variation diagram. **c** Nitric oxide variation diagram. *Significantly different from T1, $p < 0.01$

Correlations Between Δsyndecan-1 and Prognostic Indicators

Δsyndecan-1 was positively correlated with the duration of postoperative mechanical ventilation ($R = 0.318$, $p < 0.01$) and length of intensive care unit (ICU) stay ($R = 0.498$, $p < 0.01$) (Fig. 6).

Discussion

In this study, the changes in WSS showed a relationship with the degradation of glycocalyx. As expected, the WSS was negatively correlated with syndecan-1 and HS.

Acute shedding of EG caused by cardiac surgery with CPB is a complex process triggered by changes in blood flow shear stress, ischemia/reperfusion injury, inflammation/systemic inflammatory reaction syndrome (SIRS), and perioperative fluid management [16, 22]. The effects of ischemia/reperfusion on the glycocalyx could be attenuated by the blockade of xanthine oxidoreductase, which is an endogenous reactive oxygen species-producing enzyme bound to heparan sulfate domains in the glycocalyx [23]. Markus Rehm et al. [15] demonstrated that the significant increase of HS and syndecan-1 in circulation after aortic opening is caused by coronary ischemia-reperfusion injury. SIRS, which was activated by CPB, is an important factor that promotes the shedding of glycocalyx. The destruction of glycocalyx integrity can also reflect the processes of inflammation [24]. Blood flow shear stress alteration is also involved in the shedding of glycocalyx [12]. Fabio Sangalli et al. [25] noted that the shedding of the glycocalyx exposed to non-pulsatile flow is higher than that with physiological flow.

Pulsatile flow in physiological state has changed into non-pulsatile flow when performing CPB. The change of blood flow pattern during CPB results in generally decreased peak blood velocities and PWSS [18]. Similar results were observed in this study. Chronic shear stress was reported to affect the synthesis, release, and activity of proteoglycans in the glycocalyx [26]. A low WSS inhibits the synthesis of glycosaminoglycans and increases the shedding of the glycocalyx [27]. This study has observed that PWSS is negatively correlated with syndecan-1 and HS, as well as the MWSS. In addition, blood viscosity in this trial decreased significantly during CPB (Supplementary Fig. 1), which may be caused by prefilling liquid and infusion before CPB.

The glycocalyx components in the plasma, such as syndecan-1 and heparan sulfate, were used to indicate the level of glycocalyx shedding [15]. Acute degradation of the EG occurs in humans undergoing cardiac and major vascular surgery [28]. We observed that the concentrations of syndecan-1 and HS reached their peak after the aorta was unclamped. The reasons for this increase were attributed to ischemia-reperfusion injury and changes in shear stress and inflammation [15, 24, 25]. In addition, this study revealed that glycocalyx components returned to preoperative levels on the fifth postoperative day. Therefore, we suspected that the thickness of human vascular EG will recover on the fifth day after surgery. In rats, a relatively rapid regeneration of microvascular luminal glycocalyx was observed after spinal cord injury, but after 3 days, the glycocalyx indicated altered composition and charge properties [29]. In mice, full restitution of the microvascular glycocalyx occurred after 5–7 days [30]. It is maintained dynamic balance of the glycocalyx between its synthesis and degradation in physiological state. The glycocalyx component of detachment in plasma can reflect the changes in the thickness of EG.

Previous studies on the mechanisms of shear stress-induced glycocalyx shedding have not yielded a definite conclusion. Matrix metalloproteases, which are released from activated mast cells, may contribute to the shedding of syndecan-1 and heparan sulfate [31, 32]. Heparan sulfate and hyaluronic acid chains are attached to syndecan-1 and are located on the luminal surface of the glycocalyx network [33]. Matrix metalloproteases specifically cleave heparan sulfate side chains from cell surface proteins, such as syndecans and glypicans [31]. The expression of matrix metalloproteases can be upregulated by flow-induced shear stress [34]. In

Fig. 3 Individual and median change of the peak wall shear stress and mean wall shear stress at different operative stages. *Significantly different from T1, $p < 0.01$
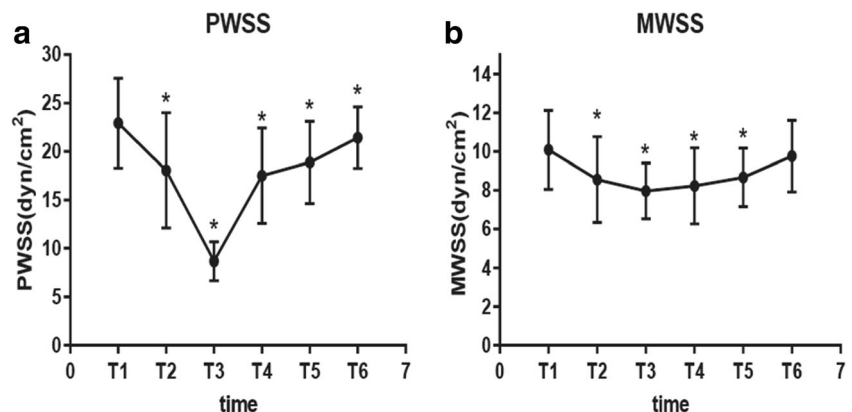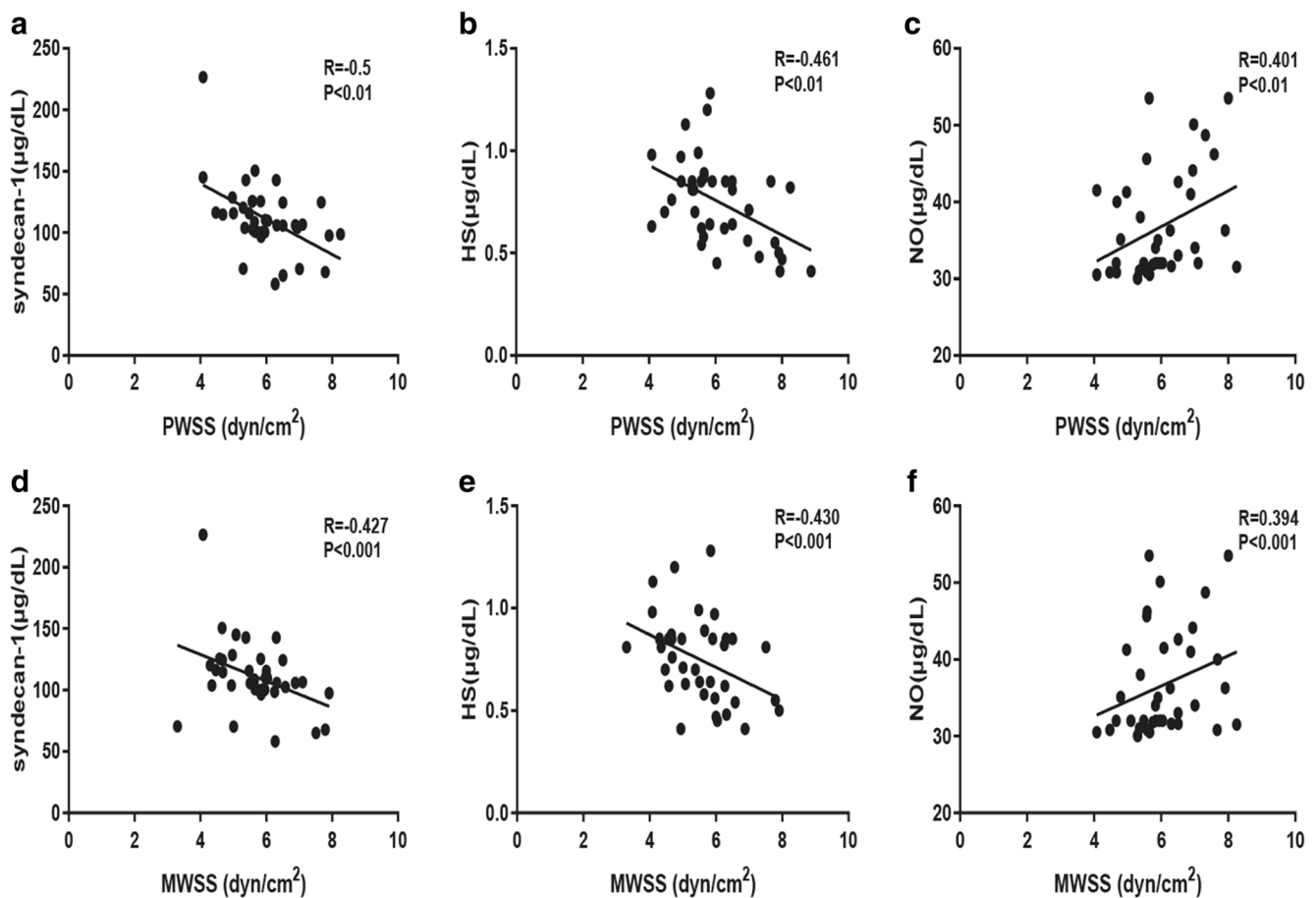
Fig. 4 Correlations of wall shear stress with heparan sulfate, nitric oxide, and syndecan-1 during CPB

addition, the amount of nitric oxide produced by shear stress-induced endothelial cells is significantly reduced due to the decreased EG in the endothelial cells [35]. In this study, the transient increases of nitric oxide can be explained by the postoperative use of exogenous nitroglycerine at T5.

A damaged EG layer can result in systemic and myocardial edema, platelet and leukocyte adhesion, and fluid extravasation and contribute to microvascular perfusion heterogeneity [16, 36]. The survival showed a significant negative

correlation with the increase in the concentrations of syndecan-1 in the plasma of individual patients [37]. The increase in serum-soluble syndecan in patients with heart failure is associated with adverse clinical outcomes, and the preservation of EG exerts a protective effect on cardiovascular systems [38]. In this study, it was found that the increase of syndecan-1 in the plasma was positively correlated with the duration of postoperative mechanical ventilation and length of ICU stay. Therefore, the timely detection and prevention of

Fig. 5 Correlation of normalized plasma levels of Δsyndecan-1 (**a**) and Δheparan sulfate (**b**) for individual patients with the aortic clamping time. Δsyndecan-1, plasma levels of T4–T1 syndecan-1; Δheparan sulfate, plasma levels of T4–T1 heparan sulfate
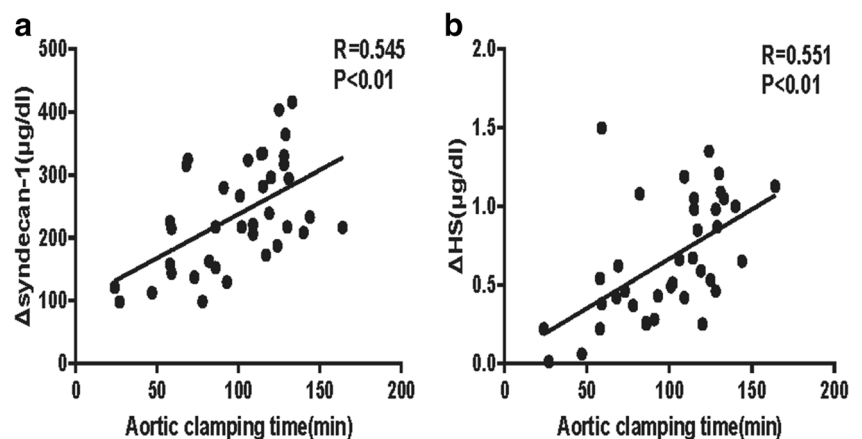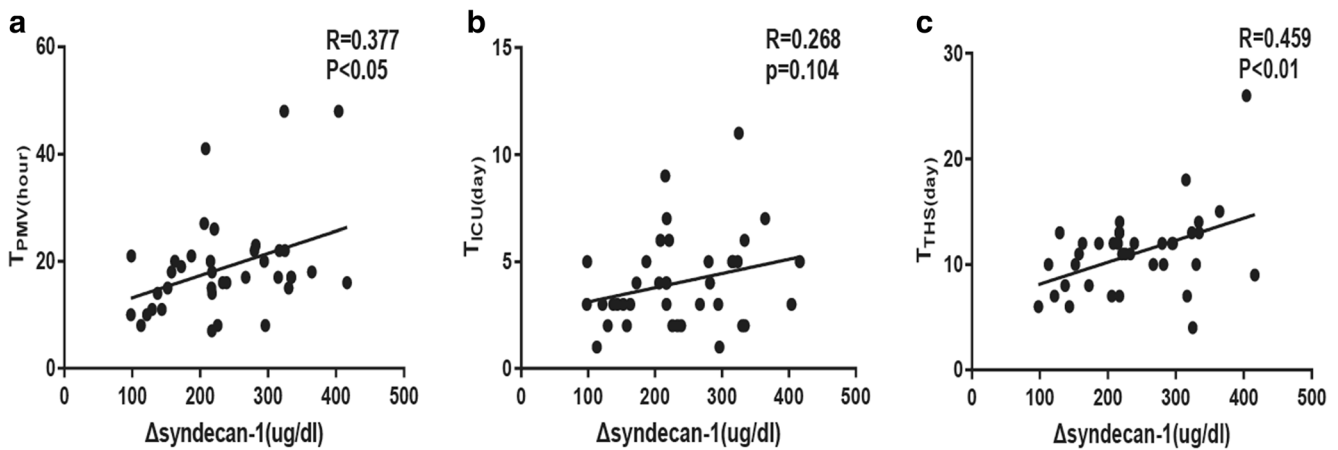
Fig. 6 Correlation of normalized plasma levels of T4–T1 syndecan-1 for individual patients with prognostic indicators. T_{PMV}, duration of postoperative mechanical ventilation; T_{ICU}, length of ICU stay; $T_{Theparan\ sulfate}$, total length of postoperative hospital stay. Δsyndecan-1, plasma levels of T4–T1 syndecan-1

damage to EG are essential for the diagnosis, treatment, and prognosis of related diseases [39]. The glycocalyx components (syndecan-1 and heparan sulfate) are available for the assessment of glycocalyx damage, but they exhibit certain limitations. Furthermore, the glycocalyx component test is invasive and expensive but fails to provide a timely reflection of the glycocalyx damage. Based on the above research, we used ultrasound measurement of wall shear stress to reflect the degree of glycocalyx shedding.

Study Limitations

This study features several limitations. First, the study only tested HS and syndecan-1, and other components, such as glypican-1 and hyaluronic acid, were excluded due to limited research funding. Moreover, considering the limitation of clinical trials, we could not use a more accurate and intuitive method such as intravital microscopy to evaluate the thickness of the glycocalyx on the surface of the vascular endothelium. In addition to WSS in CPB, the influence of inflammation, coagulation, and oxidative stress on the glycocalyx could not be eliminated during CPB.

Conclusions

It was revealed that the amount of glycocalyx shedding(syndecan-1 and HS) was significantly increased after CPB. In addition, the WSS generated by non-pulsatile flow during CPB was lower than that generated by preoperative physiological pulsatile flow. The WSS was negatively correlated with syndecan-1 and HS during CPB. These results may provide a strategy for the protection of the glycocalyx during CPB.

Compliance with Ethical Standards

References

1. Gao, L., & Lipowsky, H. H. (2010). Composition of the endothelial glycocalyx and its relation to its thickness and diffusion of small solutes. *Microvascular Research, 80*(3), 394–401. https://doi.org/10.1016/j.mvr.2010.06.005.
2. Curry, F. E., & Adamson, R. H. (2012). Endothelial glycocalyx: Permeability barrier and mechanosensor. *Annals of Biomedical Engineering, 40*(4), 828–839. https://doi.org/10.1007/s10439-011-0429-8.

3. Lipowsky, H. H. (2011). Protease activity and the role of the endothelial glycocalyx in inflammation. *Drug Discov Today Dis Models, 8*(1), 57–62. https://doi.org/10.1016/j.ddmod.2011.05.004.

4. Lipowsky, H. H. (2012). The endothelial glycocalyx as a barrier to leukocyte adhesion and its mediation by extracellular proteases. *Annals of Biomedical Engineering, 40*(4), 840–848. https://doi.org/10.1007/s10439-011-0427-x.

5. Zhang, J. X., Qu, X. L., Chu, P., Xie, D. J., Zhu, L. L., Chao, Y. L., et al. (2018). Low shear stress induces vascular eNOS uncoupling via autophagy-mediated eNOS phosphorylation. *Biochimica et Biophysica Acta, 1865*(5), 709–720. https://doi.org/10.1016/j.bbamcr.2018.02.005.

6. Bartosch, A. M. W., Mathews, R., & Tarbell, J. M. (2017). Endothelial glycocalyx-mediated nitric oxide production in response to selective AFM pulling. *Biophysical Journal, 113*(1), 101–108. https://doi.org/10.1016/j.bpj.2017.05.033.

7. Russell-Puleri, S., Dela Paz, N. G., Adams, D., Chattopadhyay, M., Cancel, L., Ebong, E., et al. (2017). Fluid shear stress induces upregulation of COX-2 and PGI2 release in endothelial cells via a pathway involving PECAM-1, PI3K, FAK, and p38. *American Journal of Physiology. Heart and Circulatory Physiology, 312*(3), H485–H500. https://doi.org/10.1152/ajpheart.00035.2016.

8. Gouverneur, M., Spaan, J. A., Pannekoek, H., Fontijn, R. D., & Vink, H. (2006). Fluid shear stress stimulates incorporation of hyaluronan into endothelial cell glycocalyx. *American Journal of Physiology. Heart and Circulatory Physiology, 290*(1), H458–H452. https://doi.org/10.1152/ajpheart.00592.2005.

9. Nikmanesh, M., Shi, Z. D., & Tarbell, J. M. (2012). Heparan sulfate proteoglycan mediates shear stress-induced endothelial gene expression in mouse embryonic stem cell-derived endothelial cells. *Biotechnology and Bioengineering, 109*(2), 583–594. https://doi.org/10.1002/bit.23302.

10. Yang, H., Zhu, L., Chao, Y., Gu, Y., Kong, X., Chen, M., et al. (2018). Hyaluronidase2 (Hyal2) modulates low shear stress-induced glycocalyx impairment via the LKB1/AMPK/NADPH oxidase-dependent pathway. *Journal of Cellular Physiology, 233*(12), 9701–9715. https://doi.org/10.1002/jcp.26944.

11. Lipowsky, H. H. (2005). Microvascular rheology and hemodynamics. *Microcirculation, 12*(1), 5–15. https://doi.org/10.1080/10739680590894966.

12. Bai, K., & Wang, W. (2014). Shear stress-induced redistribution of the glycocalyx on endothelial cells in vitro. *Biomechanics and Modeling in Mechanobiology, 13*(2), 303–311. https://doi.org/10.1007/s10237-013-0502-3.

13. Kong, X., Chen, L., Ye, P., Wang, Z., Zhang, J., Ye, F., et al. (2016). The role of HYAL2 in LSS-induced glycocalyx impairment and the PKA-mediated decrease in eNOS-Ser-633 phosphorylation and nitric oxide production. *Molecular Biology of the Cell, 27*(25), 3972–3979. https://doi.org/10.1091/mbc.E16-04-0241.

14. Yang, H., Zhu, L., Gu, Y., Kong, X., Yan, L., Chen, M., et al. (2019). Berberine inhibits low shear stress-induced glycocalyx degradation via modulating AMPK and p47(phox)/Hyal2 signal pathway. *European Journal of Pharmacology, 856*, 172413. https://doi.org/10.1016/j.ejphar.2019.172413.

15. Rehm, M., Bruegger, D., Christ, F., Conzen, P., Thiel, M., Jacob, M., et al. (2007). Shedding of the endothelial glycocalyx in patients undergoing major vascular surgery with global and regional ischemia. *Circulation, 116*(17), 1896–1906. https://doi.org/10.1161/CIRCULATIONAHA.106.684852.

16. Kaushal, S., & Wehman, B. (2015). Cardiopulmonary bypass and the endothelial glycocalyx: Shedding new light. *The Journal of Thoracic and Cardiovascular Surgery, 150*(6), 1482–1483. https://doi.org/10.1016/j.jtcvs.2015.09.071.

17. Dekker, N. A. M., Veerhoek, D., Koning, N. J., van Leeuwen, A. L. I., Elbers, P. W. G., van den Brom, C. E., et al. (2019). Postoperative microcirculatory perfusion and endothelial glycocalyx shedding following cardiac surgery with cardiopulmonary bypass. *Anaesthesia.* https://doi.org/10.1111/anae.14577.

18. Assmann, A., Benim, A. C., Gul, F., Lux, P., Akhyari, P., Boeken, U., et al. (2012). Pulsatile extracorporeal circulation during on-pump cardiac surgery enhances aortic wall shear stress. *Journal of Biomechanics, 45*(1), 156–163. https://doi.org/10.1016/j.jbiomech.2011.09.021.

19. Leguy, C. A., Bosboom, E. M., Hoeks, A. P., & van de Vosse, F. N. (2009). Model-based assessment of dynamic arterial blood volume flow from ultrasound measurements. *Medical & Biological Engineering & Computing, 47*(6), 641–648. https://doi.org/10.1007/s11517-009-0473-9.

20. Ariff, B. B., Zambanini, A., Sever, P. S., Thom, S. A., & Hughes, A. D. J. A. J. o. H. (2002). The effects of pulsatile flow on shear stress within the carotid artery., *15*(4), A68–A68.

21. Reneman, R. S., van Merode, T., Hick, P., & Hoeks, A. P. (1985). Flow velocity patterns in and distensibility of the carotid artery bulb in subjects of various ages. *Circulation, 71*(3), 500–509. https://doi.org/10.1161/01.cir.71.3.500.

22. Lerman, A., & Zeiher, A. M. (2005). Endothelial function: Cardiac events. *Circulation, 111*(3), 363–368. https://doi.org/10.1161/01.CIR.0000153339.27064.14.

23. Rubio-Gayosso, I., Platts, S. H., & Duling, B. R. (2006). Reactive oxygen species mediate modification of glycocalyx during ischemia-reperfusion injury. *American Journal of Physiology. Heart and Circulatory Physiology, 290*(6), H2247–H2256. https://doi.org/10.1152/ajpheart.00796.2005.

24. Uchimido, R., Schmidt, E. P., & Shapiro, N. I. (2019). The glycocalyx: A novel diagnostic and therapeutic target in sepsis. *Critical Care, 23*(1), 16. https://doi.org/10.1186/s13054-018-2292-6.

25. Sangalli, F., Guazzi, M., Senni, S., Sala, W., Caruso, R., Costa, M. C., et al. (2015). Assessing endothelial responsiveness after cardiopulmonary bypass: Insights on different perfusion modalities. *Journal of Cardiothoracic and Vascular Anesthesia, 29*(4), 912–916. https://doi.org/10.1053/j.jvca.2014.11.008.

26. Elhadj, S., Mousa, S. A., Biochemistry, K. F.-W. J., & J. o. C. Chronic pulsatile shear stress impacts synthesis of proteoglycans by endothelial cells: Effect on platelet aggregation and coagulation., *86*(2), 239–250.

27. Frati-Munari, A. C. (2013). Medical significance of endothelial glycocalyx. *Archivos de Cardiología de México, 83*(4), 303–312. https://doi.org/10.1016/j.acmx.2013.04.015.

28. Becker, B. F., Jacob, M., Leipert, S., Salmon, A. H., & Chappell, D. (2015). Degradation of the endothelial glycocalyx in clinical settings: Searching for the sheddases. *British Journal of Clinical Pharmacology, 80*(3), 389–402. https://doi.org/10.1111/bcp.12629.

29. Noble, L. J., Mautes, A. E., & Hall, J. J. (1996). Characterization of the microvascular glycocalyx in normal and injured spinal cord in the rat. *The Journal of Comparative Neurology, 376*(4), 542–556. https://doi.org/10.1002/(SICI)1096-9861(19961223)376:4<542::AID-CNE4>3.0.CO;2-1.

30. Potter, D. R., Jiang, J., & Damiano, E. R. (2009). The recovery time course of the endothelial cell glycocalyx in vivo and its implications in vitro. *Circulation Research, 104*(11), 1318–1325. https://doi.org/10.1161/CIRCRESAHA.108.191585.

31. Ramnath, R., Foster, R. R., Qiu, Y., Cope, G., Butler, M. J., Salmon, A. H., et al. (2014). Matrix metalloproteinase 9-mediated shedding of syndecan 4 in response to tumor necrosis factor alpha: A contributor to endothelial cell glycocalyx dysfunction. *The FASEB Journal, 28*(11), 4686–4699. https://doi.org/10.1096/fj.14-252221.

32. Mulivor, A. W., & Lipowsky, H. H. (2009). Inhibition of glycan shedding and leukocyte-endothelial adhesion in postcapillary venules by suppression of matrixmetalloprotease activity with

doxycycline. *Microcirculation, 16*(8), 657–666. https://doi.org/10.3109/10739680903133714.

33. Reitsma, S., Slaaf, D. W., Vink, H., van Zandvoort, M. A., & Oude Egbrink, M. G. (2007). The endothelial glycocalyx: Composition, functions, and visualization. *Pflügers Archiv, 454*(3), 345–359. https://doi.org/10.1007/s00424-007-0212-8.

34. Chou, P. H., Wang, S. T., Yen, M. H., Liu, C. L., Chang, M. C., & Lee, O. K. (2016). Fluid-induced, shear stress-regulated extracellular matrix and matrix metalloproteinase genes expression on human annulus fibrosus cells. *Stem Cell Research & Therapy, 7*, 34. https://doi.org/10.1186/s13287-016-0292-5.

35. Florian, J. A., Kosky, J. R., Ainslie, K., Pang, Z., Dull, R. O., & Tarbell, J. M. (2003). Heparan sulfate proteoglycan is a mechanosensor on endothelial cells. *Circulation Research, 93*(10), e136–e142. https://doi.org/10.1161/01.RES.0000101744.47866.D5.

36. Myers, G. J., & Wegner, J. (2017). Endothelial glycocalyx and cardiopulmonary bypass. *The Journal of Extra-Corporeal Technology, 49*(3), 174–181.

37. Sallisalmi, M., Tenhunen, J., Yang, R., Oksala, N., & Pettila, V. (2012). Vascular adhesion protein-1 and syndecan-1 in septic shock. *Acta Anaesthesiologica Scandinavica, 56*(3), 316–322. https://doi.org/10.1111/j.1399-6576.2011.02578.x.

38. Kim, Y. H., Nijst, P., Kiefer, K., & Tang, W. H. (2017). Endothelial glycocalyx as biomarker for cardiovascular diseases: Mechanistic and clinical implications. *Current Heart Failure Reports, 14*(2), 117–126. https://doi.org/10.1007/s11897-017-0320-5.

39. Flammer, A. J., Anderson, T., Celermajer, D. S., Creager, M. A., Deanfield, J., Ganz, P., et al. (2012). The assessment of endothelial function: From research into clinical practice. *Circulation, 126*(6), 753–767. https://doi.org/10.1161/CIRCULATIONAHA.112.093245.